BENCHMARK
Journal of Cellular Biochemistry 115:1849–1854 (2014)

Journal of Cellular Biochemistry

A Novel Segmentation-Based Algorithm for the Quantification of Magnified Cells

Gemma C. Thompson,[1] Timothy A. Ireland,[1,2] Xanthe C. Larkin,[3,4] Jonathon Arnold,[3,4] and R. M. Damian Holsinger[1,5]*

[1]*Laboratory of Molecular Neuroscience, The Brain and Mind Research Institute, The University of Sydney, Camperdown, NSW 2050, Australia*

[2]*Biomedical Technology Services, Queensland Health, Gold Coast University Hospital, Southport, QLD 4215, Australia*

[3]*Discipline of Pharmacology, School of Medical Science, The University of Sydney, Sydney, NSW 2006, Australia*

[4]*The Brain and Mind Research Institute, The University of Sydney, Camperdown, NSW 2050, Australia*

[5]*Discipline of Biomedical Science, School of Medical Sciences, Sydney Medical School, The University of Sydney, Lidcombe, NSW 1825, Australia*

ABSTRACT

Cell segmentation and counting is often required in disciplines such as biological research and medical diagnosis. Manual counting, although still employed, suffers from being time consuming and sometimes unreliable. As a result, several automated cell segmentation and counting methods have been developed. A main component of automated cell counting algorithms is the image segmentation technique employed. Several such techniques were investigated and implemented in the present study. The segmentation and counting was performed on antibody stained brain tissue sections that were magnified by a factor of 40. Commonly used methods such as the circular Hough transform and watershed segmentation were analysed. These tests were found to over-segment and therefore over-count samples. Consequently, a novel cell segmentation and counting algorithm was developed and employed. The algorithm was found to be in almost perfect agreement with the average of four manual counters, with an intraclass correlation coefficient (ICC) of 0.8. J. Cell. Biochem. 115: 1849–1854, 2014.

KEY WORDS: CELL COUNTING; QUANTIFYING CELLS; AUTOMATIC CELL COUNTING; AUTOMATED SEGMENTATION; CELL SEGMENTATION ALGORITHMS

The capability to count cells within an image of a biological sample is a necessary tool in research as well as in the diagnosis and progression of diseases in humans [McAndrew, 2004]. Traditionally, trained experts performed cell-counting manually. However, this process is tedious and unreliable due to factors such as fatigue and varying levels of experience and understanding and often leads to inconsistent results [Uemura et al., 2011]. Although manual counting is still highly valued and regularly performed, the advent of image processing technologies has given rise to many automated cell-counting methods [Fu and Mui, 1981]. These methods benefit from constant, reliable and reproducible results, vastly reduced counting times and the capability of returning additional useful data such as size, shape and density [Fu and Mui, 1981; Zhu et al., 1999; Munoz et al., 2003].

A major component of cell-counting algorithms is the method of image segmentation employed. Examples of commonly used techniques for this purpose include the circular Hough transform and watershed segmentation. However, these are by no means the only categories of image segmentation. Throughout the literature and for a diverse assortment of applications, image segmentation is widely discussed and investigated and numerous techniques have been proposed [Davis, 1975; Pal and Pal, 1993]. Examples of some

Gemma C. Thompson and Timothy Ireland contributed equally to this work.
The authors declare that they have no conflict of interest.

Grant sponsor: National Health and Medical Research Council Project; Grant number: 570982; Grant sponsor: Rebecca L. Cooper Medical Research Foundation.

*Correspondence to: R. M. Damian Holsinger, Laboratory of Molecular Neuroscience, The Brain and Mind Research Institute, The University of Sydney, Camperdown, NSW 2050, Australia. E-mail: damian.holsinger@sydney.edu.au

Manuscript Received: 25 May 2014; Manuscript Accepted: 9 July 2014
Accepted manuscript online in Wiley Online Library (wileyonlinelibrary.com): 15 July 2014
DOI 10.1002/jcb.24882 • © 2014 Wiley Periodicals, Inc.

categories of image segmentation techniques include thresholding, edge detection and region growing, all of which could be applied for cell counting purposes [Fu and Mui, 1981; Uemura et al., 2011]. However, a variety of difficulties associated with these counting algorithms have been encountered [Mouroutis et al., 1998; Bewes et al., 2008]. Many cell-counting algorithms make use of the circular Hough transform that detects objects within an image that have a circular shape [Ballard, 1981]. This technique is popular and often used successfully as cells and cell colonies are generally circular in shape. However, when images are magnified, these same cells can have irregular sizes and shapes that are more difficult to detect since image segmentation techniques operate based on common features. If cells in a magnified image do not resemble a characteristic shape, some image segmentation techniques may not recognize these structures.

In the current investigation we analysed microglial cells that had been immunohisto-chemically labelled with an antibody directed against a microglial cell surface marker. Images were captured using a 40× objective via bright field imaging on a Zeiss Laser Scanning Microscope 710 (LSM710). Microglial cells are the brains resident immune cells. Derived from macrophage cell lineage, microglia represent the central nervous systems first response to injury and their proliferation are hallmarks of pathology. The microglial cells in the images were independently counted by four investigators and the average of the manual counts were compared to automated counts that were obtained using the program ImageJ (National Institutes of Health) as well as established cell counting algorithms such as the circular Hough transform and watershed segmentation. Additional suitable image segmentation techniques were also utilised in order to compare their effectiveness. A novel cell counting algorithm was developed and tested with results compared to both manual and automated counting methods.

METHODS

TISSUE PREPARATION

Mice were deeply anaesthetised and trans-cardially perfused. Tissue was cleared with 0.9% saline solution and then fixed using 4% paraformaldehyde in 0.1 M phosphate buffer (PB). Brains were extracted and placed in the same fixative for 2 h followed by incubation overnight in a 12.5% sucrose solution in 0.1 M PB (pH 7.4, 4°C) for cryoprotection. Coronal brain sections were obtained at 40 μm intervals using a Leica CM 1900 UV cryostat at −17 °C. Sections were stored in anti-freeze (4°C) until immunoperioxidase labelling. All procedures were performed following approval of the University of Sydney Animal Ethics Committee.

IMMUNOHISTOCHEMISTRY

Sections were incubated in freezing solution at room temperature for 20 min followed by three 30-min washes in 0.1 M PB to remove freezing solution. To reduce background staining, sections were washed in 1% hydrogen peroxide and then blocked in 3% horse serum for 30 min each. Sections were incubated with primary antibody (anti-rabbit Iba-1, Wako, 1:2,000 in 0.1 M PB containing 0.1% bovine serum albumin (BSA), 2% normal horse serum and 0.2% Triton-X) overnight at room temperature. Sections were then washed in 0.1 M PB and incubated in biotinylated rabbit anti-mouse IgG (H + L) secondary antibody (Vector Labs), (1:500 in 0.1 M PB containing 0.1% bovine serum albumin (BSA), 2% normal horse serum and 0.2% Triton-X) for 1 h at room temperature, washed again in 0.1 M PB and then incubated for a further 1 h with ExtraAvidn peroxidase (Sigma, 1:1,000) followed by another 0.1 M PB wash. Sections were incubated in 0.05% 3,3-diaminobenzidine (DAB) nickel intensified (0.004% ammonium chloride, 0.02% nickel ammonium sulphate, 0.2% D-glucose), catalysed with glucose oxidase and the reaction was terminated with two washes in 0.1 M PB when deemed to be optimally stained. Sections were air-dried overnight, dehydrated through a series of graded alcohols (70%, 95%, 100%), cleared in xylene and a coverslip was applied using paramount.

IMAGE CAPTURE AND ANALYSIS

Images were examined and captured via bright-field microscopy on a Zeiss Laser Scanning Microscope 710 (LSM710) using a 40× objective.

IMAGE SEGMENTATION TECHNIQUES

A novel cell counting algorithm was tested against a number of image segmentation techniques that are often used for cell counting purposes. To assess the application of automated segmentation techniques, each image within a 97-image set was analysed. The techniques used included edge detection techniques—the Roberts [Fu and Mui, 1981; Gonzalez et al., 2004], Prewitt [Davis, 1975; Fu and Mui, 1981; Lee, 1987], Sobel [Fu and Mui, 1981; Sharifi et al., 2002], Canny [Canny, 1986; Torre and Poggio, 1986] and Laplacian of Gaussian masks, [Byun et al., 2006; Usaj et al., 2011] the Watershed segmentation technique [Safonov et al., 2006] and the circular Hough transform [Bewes et al., 2008]. The same counting function (bwlabel) was used in all of these segmentation results in order to maintain consistency.

IMAGEJ

ImageJ is a Java-based image-processing program developed by the National Institutes of Health [http://rsb.info.nih.gov/ij/download.html]. Before counting, the default threshold available in ImageJ was applied to the 97 images: Image > Adjust > Threshold. Next, the images were counted using the automated cell counter in ImageJ: Analyze > Analyze Particles.

NOVEL CELL COUNTING ALGORITHM

A novel cell counting algorithm was developed in MATLAB. A general outline of the algorithm is displayed in Supplementary Figure 1. The original 8-bit grey-scale '.png' image (pixel values from 0 to 255) was read into the MATLAB environment using the function 'imread' to obtain an MxN array with a uint8 output class. The inverse of this image was obtained by applying the Image Processing Toolbox function 'imcomplement' in order to enable efficient visual confirmation of cell count. Local histogram equalization was then applied to the image. Next, the Image Processing Toolbox function 'adapthisteq' was used to apply local histogram equalization to the image in order to enhance cell wall contrast.

Following this, the Image Processing Toolbox function 'im2bw' was applied to convert the grey-scale image to a binary image with values of 0 or 1. The binary threshold was set to 98% of maximum pixel value (in this case 242). This enabled capture of cells but also captured some noise. This noise was eliminated using the 'strel' function with the Image Processing Toolbox function 'imopen'. By creating a structuring element (strel) of 12 connected pixel values, it was possible to set an 'opening' threshold whereby any noise and debris smaller than 12 connected pixels was removed from the final image and areas of pixels greater than 12 were opened so as to fully connect what could have been incompletely sampled cells. Once again the structuring element had to be optimised for the cell sample used and this depended on the cell type, media, the number of cells and size of cell in the sample. This final binary mask leaves areas of maximum intensity that will consequently be counted as 'cells' but barely resembles the original image. The parameters used for im2bw and strel were found by applying heuristic optimisation methods based on comparison to manual cell counts from multiple counters. Cells were counted using the Image Processing Toolbox function 'bwlabel'. This function calculates all the connected components in a binary image. The general syntax is [L, num] = bwlabel(I, conn) where 'L' is a label matrix [Gonzalez et al., 2004], 'I' represents the image matrix, 'num', the number of connected matrix elements found in the image, and 'conn' identifies the number of connected elements required to be counted—either four or eight connected elements.

STATISTICS

Cell counts within each of the 97 images were recorded for the segmentation methods as well as individual counts for each of the four manual counters. The average count and standard deviation of the four manual counters was calculated and recorded as the 'average manual count'. The counts for all 97 images from each of the segmentation methods was compared individually to the 'average manual count' for a particular image in order to calculate an intraclass correlation coefficient (ICC) using ICC Model 3, k (Two-way mixed, average measure). Additionally, each of the individual manual counts for all 97 images was compared to the 'average manual count' of the image set to calculate the manual counter ICC.

RESULTS

Manual cell counts were obtained independently by four counters for 97 images. The average and standard deviation for each image from the four counters was recorded as the final manual count ± error. Table I shows the manual and novel cell count per image for a sample of 17 images.

Table I lists the results of a random sample of 17 images on which various image segmentation techniques were tested. The counted cells are highlighted (Supplementary Fig. 2) with the use of the imoverlay function developed by Steve Eddins (http://www.mathworks.com/matlabcentral/fileexchange/10502). With the exception of ImageJ, all of the other image segmentation techniques tested produced considerable over-segmentation of the images. The results from the default threshold of ImageJ were consistently below (8.0 ± 4.7) the average manual count (15.6 ± 2.8).

In order to determine the best segmentation-based algorithm, the Intraclass Correlation Coefficient (ICC) for each segmentation technique (Table II, Columns 3–11) was compared to the average manual count of 97 images (Table II). ICC analysis was chosen to estimate the overall similarity of each method compared to manual counting. The ICCs demonstrate a poor correlation between most segmentation techniques and the average manual counting method where all ICCs were rounded to a maximum value of 0.1 (Model 3, 4). As shown in Table II, only the novel segmentation (ICC 0.8 (Model 3,

TABLE I. Average Manual and Automated Cell Counting Results

	Counting technique (counted cells/image)									
Image	Manual (average)	Novel	ImageJ	Watershed	Hough	Canny	LoG	Sobel	Prewitt	Roberts
1	14.75	16	8	2,949	1,381	2,647	2,870	3,513	2,003	3,252
2	17.25	18	6	2,375	1,571	2,583	2,578	3,359	2,132	3,501
3	16.25	17	7	3,097	1,753	3,391	3,182	3,763	2,384	3,295
4	13.25	14	7	2,922	1,884	3,085	2,966	3,922	2,548	3,778
5	11.75	11	8	2,702	1,280	3,015	2,978	3,477	1,788	3,513
6	14.5	14	8	2,958	1,474	3,332	2,962	3,589	2,141	3,507
7	16.5	17	9	3,919	1,669	3,313	3,702	4,379	2,413	3,902
8	15.25	15	1	3,657	1,375	3,008	3,946	4,671	2,083	4,170
9	18.25	19	5	2,775	1,631	3,161	2,717	3,146	2,287	3,010
10	13.75	14	5	2,415	1,030	1,999	2,529	3,452	1,476	3,472
11	16.75	18	15	3,897	1,518	2,529	3,076	4,494	2,329	3,819
12	18.5	19	9	2,842	1,200	2,094	2,797	3,369	1,741	3,662
13	11.5	11	5	2,598	1,039	1,972	2,646	3,436	1,449	3,483
14	8.75	9	4	3,243	1,498	2,480	3,677	4,163	2,172	3,598
15	10.75	11	10	3,225	1,223	1,953	3,607	4,289	1,824	4,264
16	18.25	21	12	3,215	1,353	2,139	3,156	4,643	2,067	3,610
17	16	16	4	3,289	1,141	1,984	3,510	4,031	1,779	4,072

The average of four manual counters and the automated counting results for a sample of 17 images investigated.
LoG, Laplacian of Gaussian automated segmentation technique.

TABLE II. Intraclass Correlation Coefficient (ICC) Calculations

Technique	Manual	Novel	ImageJ	Watershed	Hough	Canny	LoG	Sobel	Prewitt	Roberts
ICC	0.8	0.8	0.7	<0.1	<0.1	<0.1	<0.1	<0.1	<0.1	<0.1
Agreement class	Almost perfect	Almost perfect	Strong	Poor	Poor	Poor	Poor	Poor	Poor	Poor

The ICC for each of the automated counting techniques (columns 3–11) was compared to the average manual count. Manual ICC was calculated as the average ICC of each of the counters compared to the average manual count. Column 2 represents the ICC between the four independent counters and the average manual count.

4)—almost perfect agreement) and ImageJ segmentation techniques (ICC 0.7 (Model 3, 4)—strong agreement) yielded any agreement with manual counting. This data demonstrates that the novel algorithm is a better option for successful automated segmentation and counting of the images when compared with manual counting.

The average ICC between each of the manual counters and the 'average manual count' was calculated to be 0.8 (Model 3, 1) (Table II, column 2). This suggests that the novel algorithm performed as well as any of the individual counters.

DISCUSSION

Cell counting is an important feature of many biological and medical endeavours. Increasing reliance on cell counts as readout of experimental manipulation or disease condition has necessitated the accurate and rapid counting of cells in large numbers of samples. We evaluated algorithms that are commonly used for automated cell counting and discovered that while these algorithms worked well for standard images, they performed poorly on images that were magnified. We have developed a simple, easily adaptable algorithm that demonstrates a near perfect readout when compared to manual counting.

As shown in Tables I and II, when compared to the average of four manual counters, the novel counting algorithm was capable of counting cells within the same rate of error as manual counters (ICC 0.8 for both). Additionally, Figure 1 shows that 16 out of the 17 sampled novel algorithm counts are within one SD of the average manual count. These results demonstrate that the novel counting method, once optimised, is a suitable substitute for large-scale manual cell identification and counting. Given this suitability, it is likely that improved automated segmentation techniques will replace manual counting techniques given the time efficiency, consistent counting method and minimal technical requirement of the automated techniques.

The results of a random selection of the cell counting are shown in Table I. The results of all of the image segmentation techniques are consistently higher than the manual counts; however, they are quite stable, given their magnitude. This suggests that the fundamental impediment in the application of these techniques is the image segmentation method employed. Results demonstrate that our novel algorithm is significantly better than other common segmentation

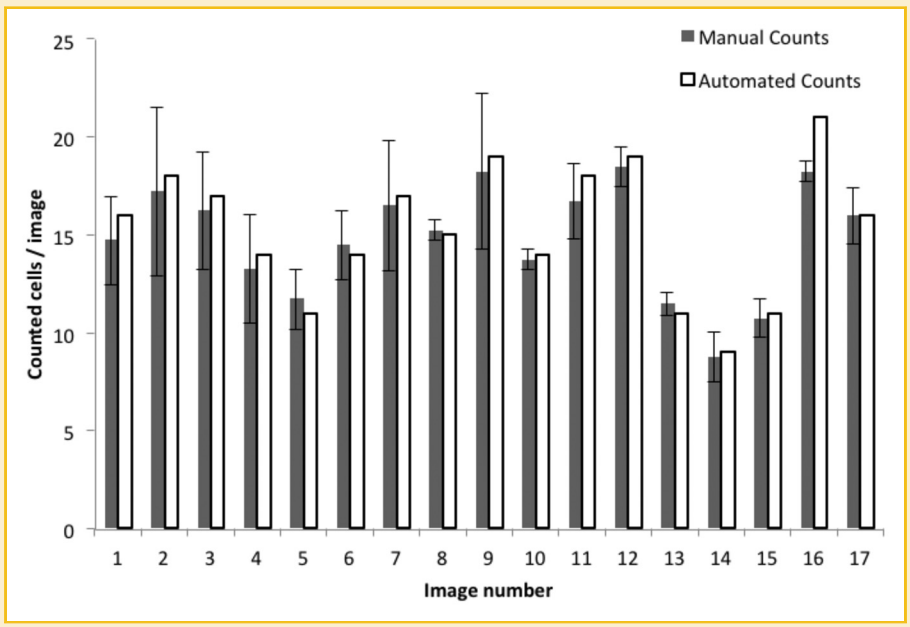

Fig. 1. Results from the novel automated counting algorithm compared to the manual counts averaged for the four manual counters with standard deviation as error. The results are for 17 out of a total of 97 images

TABLE III. Suggestions for Adaptation of the Novel Cell Counting Algorithm

Deviation	Current algorithm	Suggested change
Increased magnification	Uses strel (Structing element) of 12 connected pixels	Increase Strel size
Decreased magnification	Uses strel (Structing element) of 12 connected pixels	Decrease Strel size
Increased cell density	Uses Im2bw-Binary thresholding set to 0.98 AND Strel (Structing element) of 12 connected pixels	Optimise threshold value OR Decrease Strel size
Increased cell density	Uses Im2bw – Binary thresholding set to 0.98 AND Strel (Structing element) of 12 connected pixels	Optimise threshold value OR Increase Strel size
Different cellular shape	Uses Strel (Structing element) of 12 connected pixels AND Novel segmentation technique	Create a structuring element that matches the shape of cells OR If cells have a well-defined shape, use Hough transform and optimise the thresholding value based on goodness of fit to selected shape

The suggestions provided in this table will enable the adaptation of our novel cell counting algorithm to varying degrees of magnification, cell density and cell shape with minimal algorithm development.

algorithms tested and has a comparable intraclass correlation coefficient to that of manual counters, indicating the accuracy and reliability of the algorithm.

The result of the novel algorithm count on an image is displayed in Supplementary Figure 2 with the use of the 'imoverlay' function. This provides the means for a visual assessment of the novel algorithm's effectiveness in counting and makes evident any errors in the results of its implementation.

The programming code is provided as Supplementary Figure 3.

ALGORITHM ADAPTATION

As with many automated processes, increased accuracy requires a high level of specificity. In the current investigation, to obtain an accurate cell count under the described imaging conditions (brain tissue under 40× magnification), algorithm optimisation and specification was required. In order to use the algorithm for other applications such as for counting cells with differing morphology, increased or decreased magnification or increased cell density, optimisation will be required. Table III has been developed to enable adaptation of the algorithm structure to incorporate changes outlined above so that it could be applied to other applications with minimal algorithm development.

These adaptations are suggested starting points of algorithm modification. All changes should be tested and optimised to ensure high specificity and accuracy. The use of the MATLAB function 'imoverlay' as a mask over the original image is an efficient technique to assess if the adapted algorithm matches all cells counted by a manual counter.

CONCLUSION

The capacity to count cells in an image of a biological sample is central in many areas of science and medicine. Traditionally, this was achieved through manual counting, but recent development of automated counting algorithms that are as accurate as manual counting have made noteable contributions to the field. However, when applied to images that have been magnified, automated techniques fail due to characteristics such as magnified noise and irregular cell shape. We have developed a novel automated counting algorithm that accurately counts cells in magnified images. The results of this algorithm, when compared to the results of manual counting, were found to have an almost perfect agreement, with an ICC of 0.8. The novel algorithm was considerably more effective than any of the automated techniques applied. This algorithm is easily modified and suggestions have been provided for adaptation across numerous platforms of cell-based analysis.

INFORMATION SHARING STATEMENT

The source code for the novel cell counting algorithm described in this manuscript can be found in Supplementary Figure 3.

ACKNOWLEDGEMENTS

This work was supported by a National Health and Medical Research Council project grant (570982) and a Rebecca L. Cooper Medical Research Foundation grant to R.M.D.H.

REFERENCES

Ballard DH. 1981. Generalizing the Hough transform to detect arbitrary shapes. Pattern Recog 13:111–122.

Bewes JM, Suchowerska N, McKenzie DR. 2008. Automated cell colony counting and analysis using the circular Hough Image transform algorithm (CHiTA). Phys Med Biol 53:5991–6008.

Byun J, Verardo MR, Sumengen B, Lewis GP, Manjunath BS, Fisher SK. 2006. Automated tool for the detection of cell nuclei in digital microscopic images: Application to retinal images. Mol Vision 12:949–960.

Canny J. 1986. A computational approach to edge detection. IEEE Trans Pattern Anal Mach Intel 8:679–698.

Davis LS. 1975. A survey of edge detection techniques. Comput Graphics Image Process 4:248–270.

Fu KS, Mui JK. 1981. A survey on image segmentation. Pattern Recog 13: 3–16.

Gonzalez RC, Woods RE, Eddins SL. 2004. Digital image processing using Matlab. Upper Saddle River, NJ: Pearson Prentice Hall.

Lee JSJ, Haralick RM, Shapiro LG. 1987. Morphologic edge detection. IEEE J Robotics Autom 3:142–156.

McAndrew A. 2004. Introduction to digital image processing with Matlab. Boston, MA: Thomson Course Technology.

Mouroutis T, Roberts SJ, Bharath AA. 1998. Robust cell nuclei segmentation using statistical modelling. Bioimaging 6:79–91.

Munoz X, et al. 2003. Strategies for image segmentation combining region and boundary information. Pattern Recog Lett 24:375–392.

Pal NR, Pal SK. 1993. A review on image segmentation techniques. Pattern Recog 26:1277–1294.

Safonov IV, Mavrin GN, Kryzhanovsky KA. 2006. Segmentation of convex cells with partially undefined boundaries. Pattern Recog Image Anal 16:46–49.

Sharifi M, Fathy M, Mahmoudi MT. 2002. A classified and comparative study of edge detection algorithms. Proc Int Conf Inform Technol. Coding Comput 117–120.

Torre V, Poggio TA. 1986. On edge detection. IEEE Trans Pattern Anal Mach Intel 8:147–163.

Uemura T, Koutaki G, Uchimura K. 2011. Image segmentation based on edge detection using boundary code. Int J Innov Comput Inform Control 7:6073–6083.

Usaj M, Torkar D, Kanduser M, Miklavcic D. 2011. Cell counting tool parameters optimization approach for electroporation efficiency determination of attached cells in phase contrast images. J Microsc 241:303–314.

Zhu H, Chan FH, Lam FK. 1999. Image contrast enhancement by constrained local histogram equalization. Comput Vision Image Understanding 73:281–290.

SUPPORTING INFORMATION

Additional supporting information may be found in the online version of this article at the publisher's web-site.